Nature Environment and Pollution Technology
An International Quarterly Scientific Journal

p-ISSN: 0972-6268
(Print copies up to 2016)
e-ISSN: 2395-3454

Vol. 25 | No. 3 | Article ID B4391 | 2026

Original Research Paper

https://doi.org/10.46488/NEPT.2026.v25i03.B4391

Open Access Journal

Spatiotemporal Analysis of Long-Term Homogeneity, Meteorological Trend, and Drought Variability over the Semi-Arid Climatic Region of Bihar, India

Shashi Shekhar Pathak[1], Ravi Galkate[2], V.K. Chandola[1], Atar Singh[3], Bhupendra Joshi[1], Utkarsh Kumar[4], Rustem R. Zairov[5] and Ramesh Kumar[6]†

[1]Department of Agricultural Engineering, Banaras Hindu University, Varanasi, Uttar Pradesh, India
[2]National Institute of Hydrology (NIH Regional Center), Bhopal, Madhya Pradesh, India
[3]National Institute of Hydrology, Roorkee, Uttarakhand, India
[4]ICAR-Vivekananda Parvatiya Krishi Anusandhan Sansthan, Almora, Uttarakhand, India
[5]Arbuzov Institute of Organic and Physical Chemistry, FRC Kazan Scientific Center, Russian Academy of Sciences, 420088, Arbuzov str. 8 Kazan, Russian Federation
[6]PBS College Banka, Tilka Manjhi Bhagalpur University (TMBU), Bhagalpur, Bihar, India
†Corresponding author: Ramesh Kumar; rameshkumar9234@gmail.com

Abbreviation: Nat. Env. & Poll. Technol.
Website: www.neptjournal.com

Received: 30-08-2025
Revised: 18-11-2025
Accepted: 27-11-2025

Key Words:

Climate variability
Spatiotemporal analysis
Mann-Kendall test
Sen's slope
Drought variability

Citation for the Paper:

Pathak, S.S., Galkate, R., Chandola, V.K., Singh, A., Joshi, B., Kumar, U., Zairov, R.R. and Kumar, R., 2026. Spatiotemporal analysis of long-term homogeneity, meteorological trend, and drought variability over the semi-arid climatic region of Bihar, India. *Nature Environment and Pollution Technology*, 25(3), B4391. https://doi.org/10.46488/NEPT.2026.v25i03. B4391

Note: From 2025, the journal has adopted the use of Article IDs in citations instead of traditional consecutive page numbers. Each article is now given individual page ranges starting from page 1.

ABSTRACT

Assessing the spatiotemporal variability of meteorological parameters provides critical insights into identifying emerging environmental risks posed by climate change. Such an evaluation can help obtain strong evidence to explain the effects of climate change on crop yields and water resource management. Recent rainfall–drought studies in Bihar have advanced our understanding of seasonal variability; however, several clear research gaps remain. Most analyses still rely heavily on the Standardized Precipitation Index, overlooking complementary water balance, soil moisture, and vegetation indicators needed to capture agricultural and hydrological droughts. Therefore, this study examined rainfall and drought characteristics in the semi-arid climatic region of Bihar. The dataset was acquired from the India Meteorological Department (IMD) for the period between 1970 and 2020 at a spatial scale of 0.25° × 0.25°. Based on the change point tests, the time series was divided into two periods: 1970–1990 and 1991–2020, with 1990 as the change point year. The non-parametric Mann-Kendall test and Sen's slope were used to identify trends and estimate their magnitude at a 5% significance level. The results showed that the northwestern, southwestern, and central districts of Bihar exhibited negative trends, particularly in June, August, and September. The magnitude of the decline ranged from -1 to -2 $mm.y^{-1}$. The analysis showed an increasing trend in the total annual rainfall observed between 1970 and 2020. This pattern suggests that the methodological framework employed in this study can be effectively applied across different spatial scales and diverse geographic settings. This study provides a foundation for improved water resource management, climate adaptation planning, and strategies aimed at mitigating the potential impacts of extreme hydrological events.

1. INTRODUCTION

Climate change is a significant global challenge with consequences that affect various aspects of life (Sarkar et al. 2021, Anil & Sasi 2025). The risks and vulnerabilities created by it have complex and interconnected impacts on communities, socioeconomic systems, and natural environments (Yildirim & Rahman 2022), which in turn affect other sectors of the economy, exacerbating existing inequalities. A report by the Intergovernmental Panel on Climate Change (IPCC) indicates that the Earth's temperature is expected to increase by 1 between 2030 and 2052 (IPCC 2021). This projected warming highlights the magnitude of the risks to society and the environment. Climate variability is caused by natural variability within the climate system as well as human-made influences, including land use and land cover alterations (Belay et al. 2021, Nyembo et al. 2021). These

changes are further exacerbated by rising greenhouse gas concentrations, which have altered seasonal patterns and intensified temperature and precipitation changes on a global scale (Yürekli 2015, Khaniya et al. 2019). However, vulnerable regions are often the most severely affected, experiencing cascading effects on livelihoods, public health, and biodiversity (Asare-Nuamah & Botchway 2019). Hence, analyzing climate variability is crucial for designing effective adaptation strategies. Thus, a better understanding of such variability can lead to more effective risk management methods. When compared to other meteorological indicators, the most significant climatic parameter in the tropics, rainfall, exhibits a high degree of variability on both temporal and geographical scales. Small- or large-scale variations in precipitation can have a significant impact on water availability, leading to the shifting of animal and plant species. Additionally, variations in precipitation patterns can lead to floods and droughts (Trenberth 2011), which can affect water quality. Conversely, a reduction in precipitation may indicate an increase in the occurrence of droughts.

In the Indian context, studies have highlighted significant spatiotemporal variations in precipitation patterns, particularly during the pre-monsoon season. Previous research has indicated an increase in pre-monsoon rainfall and an escalation in dry spells across the country (Ashok et al. 2004, Dash et al. 2007). This issue has gained significant attention from both the public and policymakers (Sahana et al. 2021). Therefore, climatic variability has been extensively studied in the literature using both parametric and non-parametric approaches. However, parametric approaches are limited to normally distributed time series, and non-parametric methods may be required for non-normally distributed data. Climate change and variability have been extensively studied at various spatial scales, both regionally and globally (Wudineh et al. 2022). Many studies have analyzed rainfall patterns and variability at global, regional, and basin scales using various methods, including the Mann-Kendall test and Sen's slope (Pawar & Rathnayake 2022, Gao et al. 2022).

Bihar, a state in India, faces significant challenges from both droughts and floods, making it one of the most climate-vulnerable regions in India. With agriculture serving as the backbone of Bihar's economy and most of its population dependent on it for their livelihood, the monsoon season plays a vital role in sustaining agricultural activities in the state. However, between 2009 and 2012, the state experienced four consecutive years of droughts. In 2009 alone, 26 of Bihar's 38 districts were officially declared drought-affected, with the Magadha, Munger, Saran, and Tirhut divisions bearing the brunt of the crisis. These events highlight the state's susceptibility to climate extremes, which severely affect agricultural productivity and household income. Studies have shown a notable decrease in annual and monsoonal rainfall since the post-1960 period (Rashiq et al. 2024), in stark contrast to the increasing rainfall trend observed before 1960 (Gogoi & Rao 2022, Guhathakurta et al. 2020). Recent trends further emphasize Bihar's growing water crisis. Between 1983 and 2016, research reported a significant decline in total rainfall, a pattern that exacerbates water scarcity and intensifies the challenges of resource management. The combination of erratic rainfall patterns, recurring droughts in rural areas, and urban flooding in places such as Patna underscores the urgent need for proactive, integrated strategies to manage water resources and address climate risks. This shift signals a profound change in the region's climate dynamics, with wide-ranging consequences for agriculture, water resources, and disaster management. The rising frequency of drought-like conditions serves as a warning for future climate challenges, particularly as the state lacks a comprehensive strategy to support sustainable agricultural practices (Warwade et al. 2018, Tesfaye et al. 2017, Sharma & Priya 2023). This heightened sensitivity stems from erratic rainfall patterns, extended dry spells, and the dual threats of both flooding and drought. Analyzing rainfall trends and drought patterns in Bihar is essential for understanding the state's vulnerability to drought events. Such research can lay the groundwork for developing effective early warning systems to reduce the adverse impacts on agricultural production and household consumption of these crops. These findings also provide valuable insights for policymakers to design strategies that strengthen climate resilience and ensure food security in Bihar.

Therefore, the primary objective of this study was to conduct a comprehensive analysis of rainfall variability and assess flood and drought conditions in Bihar's Magadh Division. This study aimed to evaluate the severity of drought across the districts within the division, identify trends and change points in rainfall data, analyze the frequency and return period of droughts, and pinpoint drought-prone areas in the region. Accordingly, this study aimed to detect and quantify spatiotemporal rainfall variability and meteorological drought patterns in Bihar using a 51-year (1971–2021) gridded IMD rainfall dataset, employing multi-scale drought indices and trend analyses to ensure objective and comparable measurements. These findings underscore the need for reliable, location-specific data to anticipate and mitigate the adverse effects of climate change. By integrating research with adaptation strategies, policymakers can effectively address climate-induced vulnerabilities and develop resilient systems to safeguard the future of the region.

2. STUDY AREA

The study area for this research is the Magadh division in Bihar, formed by the Bihar State Government through the merger of four districts: Gaya, Nawada, Aurangabad, and Jehanabad (Fig. 1). Geographically, the Magadh division lies between latitudes 24°30' and 25°15' North and longitudes 84°00' and 86°03' East. The western boundary of the division is delineated by the Sone River, while the southern boundary adjoins the state of Jharkhand, which is part of Peninsular India. To the north, the Magadh division shares its boundary with the Patna division, and to the east, it is bordered by the Munger Division. This strategic geographical positioning highlights the division's significance within the broader regional framework of South Bihar and the Ganga Basin, both in terms of its natural resources and socio-economic importance. The study region has a tropical continental monsoon climate. Most precipitation occurs during the monsoon months of June to October. From November to March, fine, dry weather prevails. Winters are cold, and summers are very hot. The study region experiences an average annual rainfall of approximately 1168 mm, indicating a relatively high level of precipitation throughout the year. In terms of temperature, the area records a mean annual value of approximately 24.67°C, reflecting generally warm climatic conditions (Mishra 2020). The state features relatively flat topography and predominantly hot and humid climatic conditions, as it lies within the subtropical and temperate zones. These regions are characterized by hot, arid summers and a brief rainy season, and experience a semi-arid climate, rendering them highly vulnerable to drought. These climatic constraints pose substantial challenges to agriculture and water resource availability in the region. Recurrent droughts significantly reduce crop productivity, threatening the livelihoods of communities that depend on agricultural activities. Agriculture drives the state's economy, with rice being the dominant crop.

3. MATERIALS AND METHODS

3.1 Data Used

High-resolution gridded rainfall data were downloaded from the India Meteorological Department (IMD, Pune) at a 0.25° × 0.25° grid spacing and are available for the period 1970–2020 (51 years). The dataset was used for homogeneity analysis (detecting change points), trend analysis, rainfall variability analysis, and drought assessment. The IMD gridded rainfall dataset used in this study underwent rigorous quality control and gap-filling procedures by the IMD. As a result, the dataset contained no missing values that required further correction. Therefore, we did not perform any additional interpolation, and no data points were omitted during processing. This ensured that all analyses were based on a consistent, quality-assured rainfall record. The study area was covered by 17 grids (Table 1) at a resolution of 0.25° × 0.25°. Grids G1–G10 lie in Gaya, G11, G12, and G14 in Aurangabad, G13 and G15 in Nawada, G16 in Arwal, and G17 in Jehanabad. A workflow diagram summarizing the data processing and analysis sequence used in this study is presented in Fig. 2.

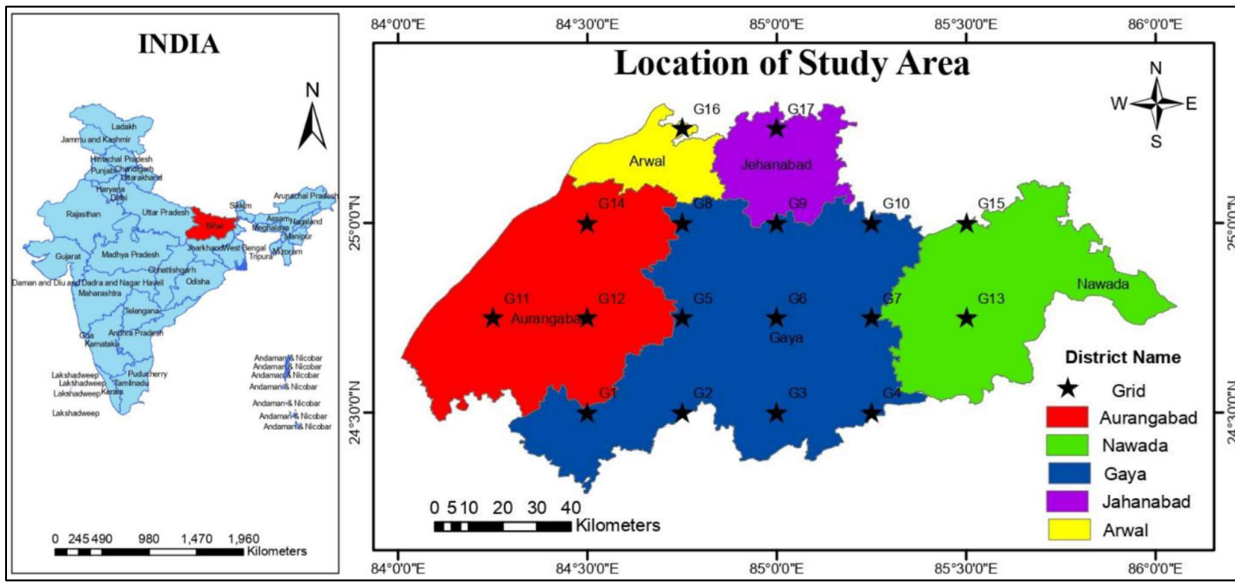

Fig. 1: Study area map showing the Magadh region with the districts of Gaya, Nawada, Aurangabad, and Jehanabad.

3.2 Homogeneity Analysis

The methodology for assessing series quality incorporated relative homogeneity tests using reference series, as outlined by Wijngaard et al. (2003), as follows: The classification criteria were a) Class A: Useful: Series that reject one or none of the null hypotheses across four tests at the 5% significance level are deemed homogeneous and suitable. b) Class B: Doubtful: Series rejecting two null hypotheses at the 5% significance level are categorized as inhomogeneous and require critical inspection before analysis. c) Class C: Suspect: Series rejecting three or all null hypotheses are classified as inhomogeneous and may be excluded from further analysis.

3.3 Pettitt's Test

This is a non-parametric test that provides an assessment of the null hypothesis (H0) and an alternative hypothesis (H1). H0 indicates homogeneous data, and H1 indicates data that cause a shift. This provides an indication of a change point when the location parameter undergoes a shift. The test statistics (Xy) used in the test are described in Equation 1:

$$\mathbf{X_y} = \mathbf{2}\sum_{i=1}^{y} r_i - y(n+1) \quad y = 1, 2, \ldots\ldots\ldots\ldots n \qquad \ldots(1)$$

The break occurs in year k when

$$X_k = \max_{1 \le y \le n} |X_y| \qquad \ldots(2)$$

The value is then compared with the critical value proposed by Pettitt (1979).

3.4 Standard Normal Homogeneity Test

The Standard Normal Homogeneity Test (SNHT) evaluates the null hypothesis (H0), which assumes that the dataset is homogeneous, against the alternative hypothesis (H1), which proposes that a notable shift occurs in the location parameter at a specific point in time, labelled moment y. To assess this, the test uses the statistic T(y), which compares the average of the initial y observations with the average of the remaining (n–y) observations. This can be expressed by Equation 3:

$$T_y = y\bar{z}_1 + (n-y)\bar{z}_2 \, , y = 1,2, \ldots\ldots\ldots\ldots n \qquad \ldots(3)$$

where $\bar{z}_1$ and $\bar{z}_2$ are the average values of the observed feature before and after *y*:

$$\bar{z}_1 = \frac{1}{y}\sum_{i=1}^{n} \frac{(Y_i - \bar{Y})}{s} \qquad \ldots(4)$$

$$\bar{z}_2 = \frac{1}{n-y}\sum_{i=y+1}^{n} \frac{(Y_i - \bar{Y})}{s} \qquad \ldots(5)$$

The year y is identified as the break year if the value of T(y) reaches its maximum value. The null hypothesis is rejected if the test statistic T(y) exceeds the critical value, which is determined based on the sample size.

$$T_0 = max_{1 \le y \le n} T_y \qquad \ldots(6)$$

3.5 Buishand`s Test

It is a non-parametric method used to determine whether a change point occurs within a dataset, indicating a shift in the location parameter. Under the null hypothesis (H_0), the data are considered homogeneous with no change point present, whereas the alternative hypothesis (H_1) indicates that a change point exists. The adjusted partial sum is expressed as follows (Equation 7):

$$S_0^* = 0 \; and \; S_y^* = \sum_{i=1}^{y} (Y_i - \bar{Y}) \quad y = 1, 2, \ldots\ldots\ldots\ldots n \qquad \ldots(7)$$

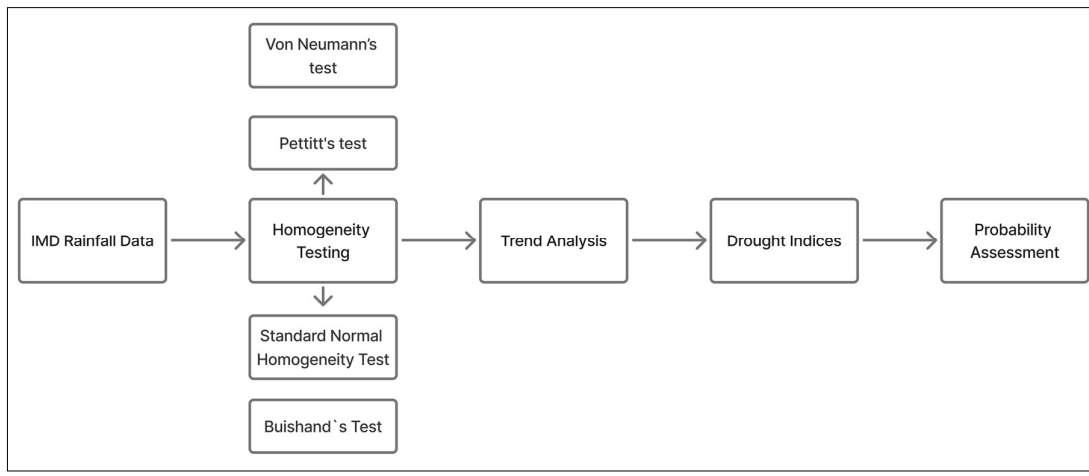

Fig. 2: Workflow diagram illustrating the data processing and analysis sequence, beginning with the IMD gridded rainfall data and proceeding through homogeneity testing, trend analysis, drought index computation, and probability assessment.

When the series is homogeneous, the value of S_y^* fluctuates around zero. A break in year y is identified when S_y^* reaches its maximum (indicating a negative shift) or minimum (indicating a positive shift). The rescaled adjusted range, R, is calculated as

$$R = \frac{(max_{0\le y\le n}S_y^* - min_{0\le y\le n}S_y^*)}{s} \quad \ldots(8)$$

$R/\sqrt{n}$ is then compared with the critical values given by Buishand (1982).

3.6 Von Neumann's Test

This method evaluates variability by comparing the mean square of successive (year-to-year) differences with the overall variance of the dataset. This comparison forms the basis of the test statistics, which can be mathematically expressed as follows (Equation 9):

$$N = \frac{\sum_{i=1}^{n-1}(Y_i - Y_{i+1})^2}{\sum_{i=1}^{n}(Y_i - \bar{Y})^2} \quad \ldots(9)$$

When the data sequence is homogeneous and does not change, the expected value of E(N) is 2. In contrast, the presence of a structural break within the sample reduces the value of N to below 2. If the computed value of N remains close to or above 2, this suggests that the observed fluctuations are the result of frequent short-term shifts in the mean, rather than a clearly defined structural break in the series.

3.7 Trend Analysis

Trend analysis refers to systematic changes observed in a variable over time, which can be identified using parametric and non-parametric statistical techniques. The precipitation data were prepared as seasonal time series: annual monsoon (June–September), pre-monsoon (March–May), post-monsoon (October–December), and winter (December–February), to examine potential seasonal variations. One of the widely applied approaches for detecting such trends in climatology and hydrology is the Mann–Kendall test, which is a non-parametric statistical method. The Mann–Kendall (MK) test and Sen's slope estimator were cross-validated using a consistent significance criterion. A two-tailed significance level of $\alpha = 0.05$ was applied using the critical threshold to determine the presence of a statistically significant trend. Sen's slope was then calculated as the median of all pairwise slopes, and its 95% confidence interval was determined. A trend was accepted as significant only when the MK test indicated significance at α=0.05, and the confidence interval of Sen's slope did not include zero, ensuring consistent cross-validation of direction and magnitude. In this test, the null hypothesis (H_0) assumes the absence of any trend, whereas the alternative hypothesis (H_1) indicates the presence of a significant trend.

Considering a dataset with n observations (x_1, x_2, x_3, …, xn), the Mann–Kendall test statistic S is defined as follows:

$$S = \sum_{i=1}^{n-1}\sum_{j=i+1}^{n} sgn\left(x_j - x_i\right) \quad \ldots(10)$$

where n is the number of observations, xj denotes the jth observation, and sgn (θ) refers to the sign function, which is defined as follows:

$$Sgn(\theta) = \begin{cases} 1 & if\ \theta > 0 \\ 0 & if\ \theta = 0 \\ -1 & if\ \theta < 0 \end{cases} \quad \ldots(11)$$

Assuming that the data follow an independent and identically distributed pattern, the expected value and variance of the S statistic can be expressed as

$$E[S] = 0 \quad \ldots(12)$$

$$Var(S) = \frac{N(N-1)(2N+5) - \sum_{k=1}^{n} t_k(t_k-1)(2t_k+5)}{18} \quad \ldots(13)$$

Z-statistics can be computed as follows:

$$Z = \begin{cases} \frac{S-1}{\sigma} & if\ S > 0 \\ 0 & if\ S = 0 \\ \frac{S+1}{\sigma} & if\ S < 0 \end{cases} \quad \ldots(14)$$

The null hypothesis was evaluated at a significance level of 5%. A positive Z-value indicates an upward trend, whereas a negative Z-value indicates a downward trend.

Sen's slope technique is commonly applied to estimate the magnitude of trends in hydro-meteorological time series. The slope (Ti) of each pair of data was computed as follows:

$$T_i = \frac{x_j - x_k}{j-k} \quad for\ i = 1,2,\ldots\ldots\ldots N \quad \ldots(15)$$

where xj and xk are the data values at times j and k (j > k), respectively.

3.8 Assessment of Metrological Drought

The meteorological drought aspects of the study area were analyzed using rainfall data. A rainfall departure analysis was performed to assess drought occurrence and measure annual rainfall shortfalls. A particular year was considered a drought year if the recorded annual rainfall in that area was more than 25% below the long-term average (Keyantash & Dracup 2002). For the Magadh Division, this analysis was conducted using rainfall records spanning 51 years (1970–2020) across all 17 grids in the region. Based on this dataset, drought years were identified and the mean frequency of droughts

was estimated. The annual departure analysis included the following steps:

a) Determination of mean (Xm) for a set of n annual rainfall data x. Xm = sum of x divided by n

b) Calculate departure (Di) by subtracting the mean (Xm) from the individual annual rainfall, Di = Xi –Xm

c) Calculate the departure percentage (Di)% = Di/Xm

In this study, drought severity was classified based on the percentage deviation from normal rainfall into the following severity classes:

a) Moderate drought: percentage annual rainfall departure between 25 and 50 percent

b) Severe drought: percentage annual rainfall departure between 50 and 75 percent

c) Extreme drought: percentage of annual rainfall departure greater than 75 percent.

3.9 Probability Distribution of Annual Rainfall

Assessing the probability distribution of yearly rainfall is crucial for estimating the frequency of different rainfall ranges with a high degree of accuracy and reliability. To identify drought-prone areas within the Magadh region, the likelihood of receiving at least 75% of the average annual rainfall was calculated. According to the guidelines of the Central Water Commission (CWC), a region is classified as drought-prone if the probability of receiving 75% of normal rainfall is below 80%. The drought categories used in this study followed the official IMD classification based on rainfall anomaly percentages and the CWC guidelines for hydrometeorological drought assessment. Accordingly, rainfall departures between –19% and –25% were classified as 'moderate drought,' and departures below –25% as 'severe drought,' and the corresponding SPI-based thresholds were aligned with the IMD/CWC definitions. The probability of the distribution of annual rainfall was analyzed using the following procedure:

a) Computation of mean rainfall at each grid, $X_m = \frac{\sum(x)}{n}$

b) The dataset was arranged in descending order based on rainfall magnitude.

c) Ranking the dataset, that is, m = 1,2,3, up to the last rainfall record.

d) Determination of cumulative probability by Weibull's formula, which is given as

$$P = \frac{m}{n+1} \times 100$$

e) Calculated probability based on 75 percent of the normal rainfall data, i.e.,

$$P_{75} = X_m \times \frac{75}{100}$$

If P75 is less than 80 percent, the area is considered drought-prone; if P75 is greater than 80 percent, the area is not considered drought-prone.

4. RESULTS AND DISCUSSION

The analysis of rainfall trends over the semi-arid climatic region of Bihar revealed a complex pattern of changes across different seasons. Long-term trend analysis from 1970 to 2020 indicated a significant decrease in annual and monsoon rainfall. This declining trend is consistent with the findings of other studies, which also reported a significant reduction in annual and monsoon rainfall, particularly after a shift change point. The variability in rainfall patterns is further complicated by high coefficients of variation (CV) for the pre-monsoon, winter, and post-monsoon seasons across all districts, indicating significant spatial and temporal variability (Singh et al. 2024a). Innovative trend analysis suggests either no trend or a negative trend in most districts, with recent years showing a more pronounced negative trend (Singh et al. 2024b). However, departure and probability distribution analyses focused exclusively on the southwest monsoon and annual rainfall across all grids. The analysis utilized 51 years (1970–2020) of data from the Indian Meteorological Department (IMD). Rainfall components are critical for drought management and planning purposes. Departure and probability distribution analyses were applied to assess drought frequency and return periods, and to identify drought-prone grids. Trend analysis and correlation were conducted using the non-parametric Mann-Kendall test, while Sen's slope estimator quantified the magnitude and percentage of slope changes.

4.1 Homogeneity Test

The reliability of climatic data is crucial for hydrological and meteorological analyses, and detecting inhomogeneities is a key step in ensuring data quality (Ribeiro et al. 2016, Singh et al. 2024a). Several studies have emphasized the complementary nature of these tests. By employing multiple tests, a study can gain a more comprehensive understanding of data integrity. However, the variation in the test results also underscores the need for further investigation to corroborate the findings and understand the specific causes of the detected inhomogeneities, such as natural climatic variability or changes in observational practices. Thus, Pettitt's, SNHT, Buishand's, and von Neumann (VN) tests were applied to test homogeneity and to determine the probable change year. The findings illustrate the homogeneity test for the annual rainfall series of the Magadh Division (Table 1). The

Table 1: Grid number with respect to the latitude and longitude values of the study area district.

Serial No	Grid No	Latitude	Longitude	District
1	G1	24.5	84.5	Gaya
2	G2	24.5	84.75	Gaya
3	G3	24.5	85	Gaya
4	G4	24.5	85.25	Gaya
5	G5	24.75	84.75	Gaya
6	G6	24.75	85	Gaya
7	G7	24.75	85.25	Gaya
8	G8	25	85.75	Gaya
9	G9	25	85	Gaya
10	G10	25	85.25	Gaya
11	G11	24.75	84.25	Aurangabad
12	G12	24.75	85.5	Aurangabad
13	G13	24.75	85.5	Nawada
14	G14	25	85.5	Aurangabad
15	G15	25	85.5	Nawada
16	G16	25.25	84.75	Arwal
17	G17	25.25	85	Jehanabad

analysis revealed that among the 17 analyzed grids, different statistical homogeneity tests yielded varying results regarding the inhomogeneity of the annual precipitation data. The semi-arid climatic region of Bihar, India, exhibits significant variability in meteorological trends and drought patterns, which are influenced by both natural and anthropogenic factors. The analysis of precipitation trends from 1970 to 2020 revealed a moderate coefficient of variation (CV) and standard deviation (SD) for both monsoon and annual rainfall, with higher variability observed in the pre-monsoon, winter, and post-monsoon seasons across districts, except for Begusarai and Jahanabad (Singh et al. 2024b).

Pettitt's test and the Standard Normal Homogeneity Test (SNHT) identified three grids (G5, G10, G15) and two grids (G7, G15), respectively, as being inhomogeneous. In contrast, Buishand's test and the Von Neumann ratio test (VN) indicated a higher number of grids with inhomogeneity, identifying six (G4, G5, G7, G8, G10, and G15) and seven grids (G3, G4, G6, G7, G9, G13, and G15), respectively. The variability in the results highlights the unique sensitivity and focus of each test in identifying inhomogeneities within the climatic datasets. Pettitt's and SNHT tests are particularly adept at detecting abrupt shifts or single change points in data, which may explain why they flagged fewer grids than the other tests. These methods are particularly effective for identifying step changes caused by factors such as station relocation, changes in instrumentation, or sudden climatic anomalies. The Buishand test is tailored to assess shifts in the mean over time, whereas the Von Neumann (VN) test evaluates the randomness of data to identify broader inconsistencies. Their ability to capture trends or gradual shifts likely explains why they identified a greater number of grids as being inhomogeneous. The VN test flagged the highest number of inhomogeneous annual rainfall data series, reflecting its sensitivity to deviations from homogeneity in the dataset. However, it is important to note that the VN test only determines whether the data series is serially correlated by testing the null hypothesis; it does not pinpoint the specific year in which the change occurred. In contrast, Pettitt's test, a non-parametric method widely used for detecting change points in hydrological and climatological studies, identified the probable years of change for the rainfall data series in grids G5, G10, and G15 as 1990, 1990, and 1991, respectively. This difference highlights the complementary utility of these statistical methods, where the VN test offers a preliminary screening for serial correlation, and Pettitt's test provides temporal localization of abrupt changes within the dataset. The Standard Normal Homogeneity Test (SNHT) identified 1987 and 1991 as the years of significant change for stations G7 and G15, respectively. Similarly, the Buishand Range Test revealed change points for multiple stations: G4 in 1987, G5 in 1990, G7 in 1989, G8 in 2003, G10 in 1990, and G15 in 1991. These tests indicate temporal shifts in the homogeneity of climatic or hydrological data, reflecting possible changes in environmental factors, measurement practices, or regional climatic dynamics during these periods (Zhang et al. 2013). Fig. 3 shows the probable change-point years identified in the annual rainfall series, determined through various homogeneity tests.

These results highlight significant shifts in rainfall patterns, which align with findings from previous research (Vicente Serrano et al. 2020, Wen et al. 2020, Saharwardi et al. 2022, Chong et al. 2022) on climatic variability and long-term hydrological trends. The detection of change points using multiple statistical tests strengthens the reliability of these observations, providing critical insights into the temporal variations in precipitation (Praveen et al. 2020). Thus, while planning water resources and monitoring droughts and floods in the area, priority should be given to G15, followed by G7. According to the Wijngaard classification framework, the annual precipitation data series for the Magadh Division was evaluated, revealing significant insights into grid-level reliability. The analysis identified 12 grids (G1, G2, G3, G5, G8, G9, G11, G12, G13, G14, G16, and G17) as "useful," indicating robust and reliable precipitation records at these locations. Conversely, grids G4, G5, and G10 were categorized as "doubtful," suggesting inconsistencies or limitations in data quality that necessitate further scrutiny. Additionally, two grids, G7

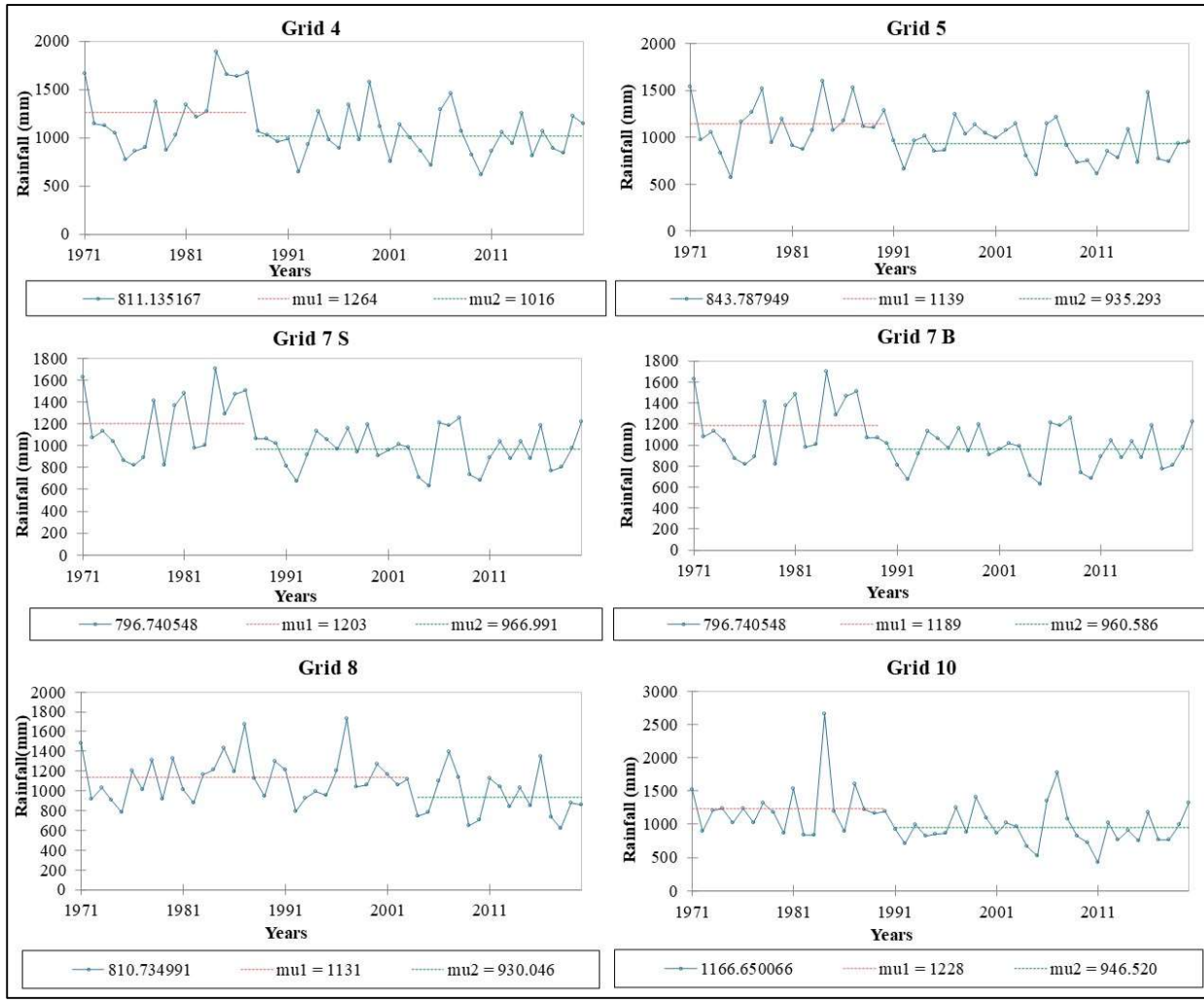

Fig. 3: Change year in annual rainfall in G4, G5, G7, and G8 by Buishand's test (mu1 and mu2 represent the mean rainfall before and after the change point, respectively). Change the year in the annual rainfall in G7 using the SNHT test. Change the year in the annual rainfall in G10 by Pettitt's and Buishand's tests.

and G15, were classified as "suspect," indicating potential anomalies or significant deviations in the precipitation records that could undermine their reliability (Larsen & Schönhuber 2018). Given these findings, strategic water resource planning and effective management of drought and flood risks in the Magadh Division should be prioritized in G15, followed by G7, owing to their critical classification. The homogeneity test of the total annual rainfall time series in the study area indicated that 71% of the stations were assigned to Class 1, 'useful', and 83% of the stations were found to be homogeneous at a significance level of 5%. Non-homogeneous stations for the years 1987-88 (G4), 1990-91 (G5), and 1990-91 (G10) are regarded as 'doubtful', while inhomogeneous stations for the year 1987-88 (G7) and 1991-92 (G15) are rated as 'suspect.' The spatially coherent change points around 1990–1991 likely reflected a large-scale climatic shift rather than isolated grid-level anomalies. This period coincides with several well-documented regional and global climate changes, including a transition in the Indian Summer Monsoon circulation, marked by altered monsoon depressions and moisture transport patterns. These broad-scale drivers can produce synchronized hydroclimatic responses across adjacent grids, thereby explaining the strong spatial coherence in the detected change years across Bihar. These grids require enhanced monitoring efforts, including the installation of more precise data collection systems, periodic reassessment of meteorological records, and integration with advanced hydrological modelling techniques (Sudriani et al. 2023). Such focused attention will help address uncertainties in precipitation patterns,

ensuring accurate forecasting and effective decision-making in regional water resource management.

4.2 Variability in Annual Rainfall Pattern (1970-2020)

The rainfall statistics for the entire study period (1970-2020) across all 17 grids in the Magadh Division are presented in Table 2. The results suggested that the maximum and minimum rainfall (mm) between different grids in winter (26.8 and 21.3), pre-monsoon (64.3 and 33.2), SW-monsoon (927.8 and 812.0), and post-monsoon (84.9 and 50.4) seasons, respectively. The maximum and minimum annual rainfall in the study area were recorded as 1094.7 mm and 930.9 mm, respectively. The results show that the annual average rainfall varies from 930.9 mm in the western region to 1094.6 mm in the eastern and southern parts of the study area. The average annual rainfall (AAR) in the study region is estimated to be 1,010.6 mm. Analysis of the rainfall distribution indicated that nearly half of the area, approximately 47%, received an annual total rainfall (ATR) below the mean value (Fig. 4a). Based on the mean and standard deviation of different time series, the highest coefficient of variation (CVs) in rainfall was found in winter, that is, 126.7%, and the lowest CV was found in the annual series, that is. 21.5%. The CVs for the SW-Monsoon data series ranged from 38.3% at grid 10 to 22.6% at grid 11, which follows the CV of the annual data series, that is, 33.5% at G10 and 21.5% at G11.

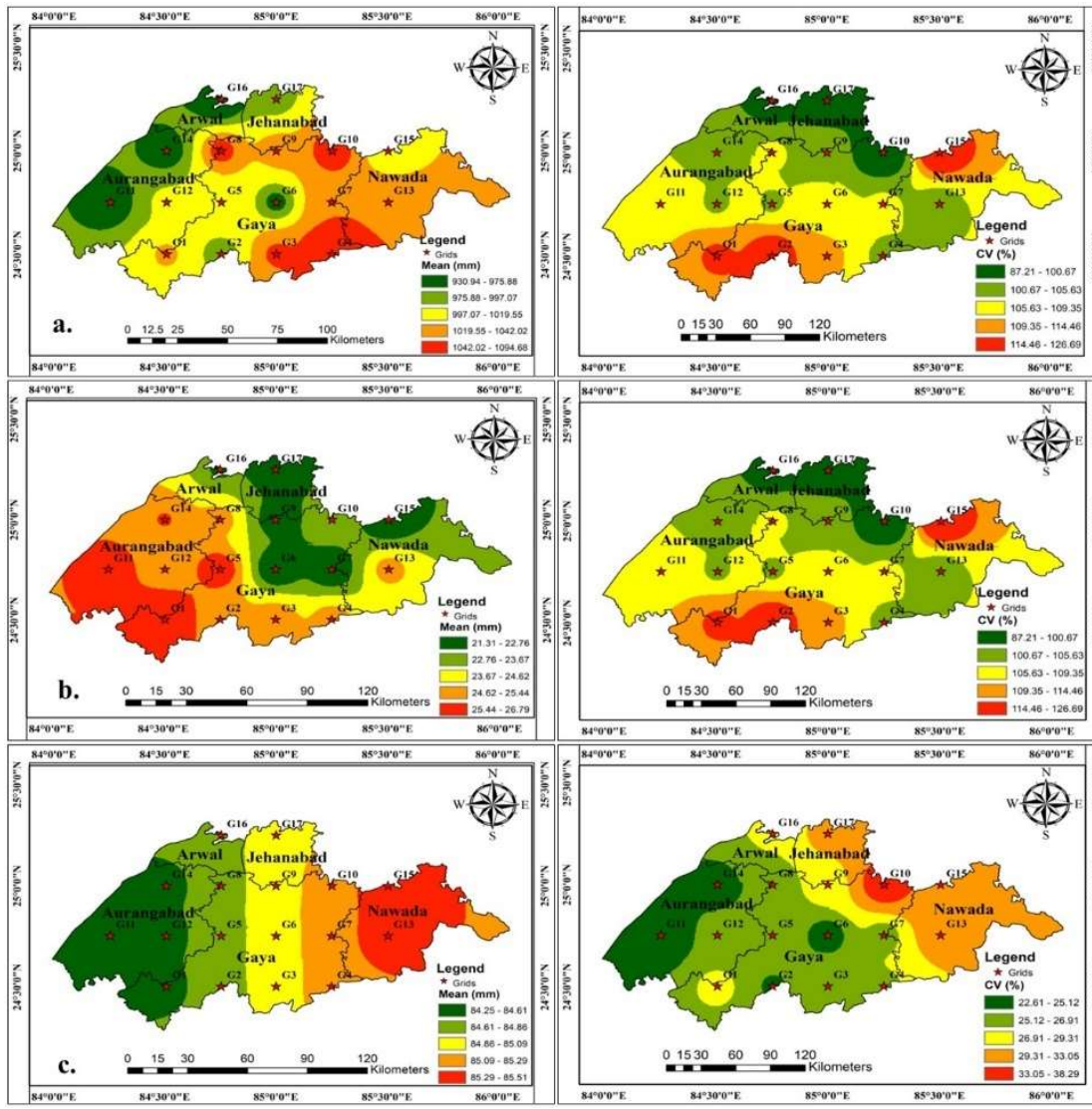

Fig. 4: a. Average annual rainfall and coefficient of variation in percentage. Mean winter rainfall and coefficient of variation (CV) in percentage. The mean southwest monsoon rainfall and CV with areal coverage in the study area between 1970 and 2020.

The findings demonstrated that there was more variability in rainfall over the Magadh Division during winter, followed by post-monsoon, pre-monsoon, SW-monsoon, and annual (Table 2). This could be due to the lower and non-uniform rainfall received during winter compared to the SW monsoon and annual rainfall. The analysis of the rainfall statistics in Table 2 reveals that the grids with heavy and frequent uniform rainfall exhibit the least variability, that is, 12.0% annually. In contrast, zones of lower rainfall were associated with higher variability in winter, at 39.5%. In addition, the results showed that the mean rainfall in the winter season varied from 21.3 mm in the middle part to 26.7 mm in the western and southern parts of the study area (Fig. 4b). The mean rainfall in the winter season for the entire study area was 24.1 mm, and 41% of the region had less than the mean rainfall in the study area. However, in the South-West monsoon, the mean rainfall is 812-927 mm with an average rainfall of 872 mm over the entire study period from to 1970-2020 (Fig. 4c). The variability found in the rainfall over the entire study area during the study period focuses on the need to find trends in different data series (Zakwan & Ara 2019, Gupta et al. 2022).

4.3 Variability in the Rainfall Pattern in the South-West (SW) Monsoon

For the southwest (SW) precipitation data series, the homogeneity of 17 spatial grids was evaluated using multiple statistical tests. Pettitt's and the Standard Normal Homogeneity Test (SNHT) identified grid G15 as exhibiting inhomogeneities. In contrast, Buishand's Range Test detected three grids, G4, G7, and G15, as inhomogeneous. Additionally, the Von Neumann Ratio (VNR) test showed that four grids, G3, G4, G7, and G13, demonstrated significant deviations from homogeneity. These results underscore the variability in detecting inhomogeneous grids across different statistical methods, emphasizing the necessity for a comprehensive approach to ensure the reliability of precipitation datasets in climate research and hydrological modeling (Vahab & Sankaran 2025). Pettitt's and SNHT tests identified 1991 as a significant change-point year at grid G15, indicating a possible shift in climatic or hydrological conditions. Furthermore, Buishand's test detected additional change points: 1987 at grid G4 and 1988 at G7. Analyzing the reliability of these grids using Wijngaard's classification revealed that most grids were reliable, except for G4 and G7, which were classified as doubtful, and G15, which was categorized as suspect. Despite this classification, G15 emerged as the most critical grid within the Magadh Division, warranting prioritized attention for water resource planning, particularly in the monsoon season. These findings underline the importance of robust grid-level analyses for developing targeted and effective water management strategies, as shifts in hydrological regimes can have profound implications for resource allocation and climate resilience. Previous research

Table 2: Rainfall statistics for the Magadh region were analyzed across 17 grids categorized by seasonal patterns: winter, pre-monsoon, southwest monsoon, post-monsoon, and annual rainfall.

Grid No	Winter		Pre-Monsoon		SW- Monsoon		Post-Monsoon		Annual	
	Mean	CV	Mean	CV	Mean	CV	Mean	CV	Mean	CV
G1	26.78	116.02	37.88	88.15	885.23	27.85	73.56	84.18	1023.5	25.5
G2	24.97	122.89	39.23	89.09	855.41	24.86	64.64	85.52	984.25	24.44
G3	25.4	110.74	49.29	90.22	893.84	26	78.81	72.94	1047.34	26.72
G4	25.16	104.58	64.34	86.88	920.28	26.5	84.91	81.56	1094.69	26.46
G5	26.3	104.66	44.97	80.24	874.17	26.4	68.07	83.71	1013.51	24.45
G6	21.33	108.26	44.66	86.31	831.8	23.47	65.85	89.16	963.64	22.89
G7	21.58	106.37	59.07	89.54	892.84	25.54	68.85	85.05	1042.34	23.75
G8	25.06	106.95	44.4	79.32	927.8	25.1	60.31	94.27	1057.57	23.19
G9	22.07	104.26	55.06	103.49	891.78	27.9	61.21	100.38	1030.13	26.95
G10	23.5	87.2	60.8	76.3	907.2	38.3	69.9	87.5	1061.4	33.5
G11	25.9	107.1	33.2	84.9	838	22.6	57.1	84	954.3	21.5
G12	25.1	104.8	43.4	76.1	870.9	25.7	62.9	81.8	1002.2	23.4
G13	25.1	102.5	55.9	78.4	880.4	31.4	71.3	84.4	1032.7	30
G14	25.5	103.3	39.5	77.4	840.1	24	51.1	85.8	956.2	22.2
G15	21.6	126.7	53.6	93.4	859.5	33	65	94.2	998.3	30.9
G16	22.6	95.9	45.9	79.3	812	27.3	50.4	99.2	930.9	25.5
G17	21.8	95	53.1	78.3	856.1	30.9	56.7	91.9	987.7	28.5

has also reported that the variability in the rainfall patterns of the southwest monsoon in Bihar from 1901 to 2020 indicates notable shifts in seasonal rainfall distribution, with a marked increase in daily rainfall intensity during the monsoon season, particularly in northern Bihar (Rashiq et al. 2024, Tiwari & Sarthi 2024, Kumar et al. 2022). Further research focusing on the period from 1950 to 2016 revealed a declining trend in monthly, seasonal, and annual rainfall, except for May, which exhibited an increasing trend (Guhathakurta et al. 2020). The study also reported high intra- and inter-annual variability, with an average coefficient of variation of 91.26%, and a significant concentration of rainfall (84%) during the monsoon months (Zakwan & Ara 2019). Additionally, a substantial decline in total rainfall over the last three decades (1986–2016) was observed, underscoring the need for effective rainwater harvesting and management strategies to mitigate potential water shortages in the region. These results highlight the identified probable change years, indicating potential shifts or anomalies in the dataset. The detected change years are further visualized in Fig. 5, which provides a comparative representation that enhances clarity and supports pattern recognition. This integrative approach combines statistical and graphical methods to ensure a comprehensive understanding of the spatial and temporal variations in the data, as supported by relevant studies that emphasize the importance of homogeneity analysis in detecting climate trends and anomalies.

4.4 Mann-Kendall Test-Based Trend Analysis and Change Percentage

During the homogeneity analysis of the annual data series, the change point was found to be quite variable, but the most probable change year was 1990, as observed by different tests over two grids, that is, G5 and G10. Since the most probable change year is 1990, the entire data series was divided into two parts by breaking the series before and after 1990. Thus, three data time series were obtained, namely TS1, TS2, and TS3, for the year 1970-2020. 1970-1990 and 1991-2020, respectively. The Mann-Kendall test was applied to monthly rainfall data for different time periods, that is, annual, winter, pre-monsoon, and post-monsoon periods, to detect significant and non-significant trends in all three series of data at a 95% significance level. The percentage change in rainfall was also determined.

4.4.1 Trend Analysis and Change Percentage for TS1 (1970-2020)

The Mann-Kendall test was applied to the monthly rainfall data for different periods of the first time series (TS1) for all grids, and the corresponding Z values. The corresponding table also contains the percentage change in rainfall calculated using the mean for all periods at each grid point. The findings suggest that almost all grids and periods exhibit a negative or positive trend, except for G3, which shows no trend during the monsoon. Moreover, a significant negative trend was observed at G5 in both the annual and monsoon rainfall periods, with Z values of -2.18 and -2.08, respectively. A similar significant negative trend was observed at G10 and G15 for both periods, with Z values of -2.57, -2.18, and -2.08, -2.0, respectively. A positive significant trend was observed for the pre-monsoon period, with a Z value of 2.39, and a negative significant trend was observed in the post-monsoon period, with a Z value of -2.01 at G9. No significant trends in winter season rainfall were observed at any grid. The findings suggested that the highest

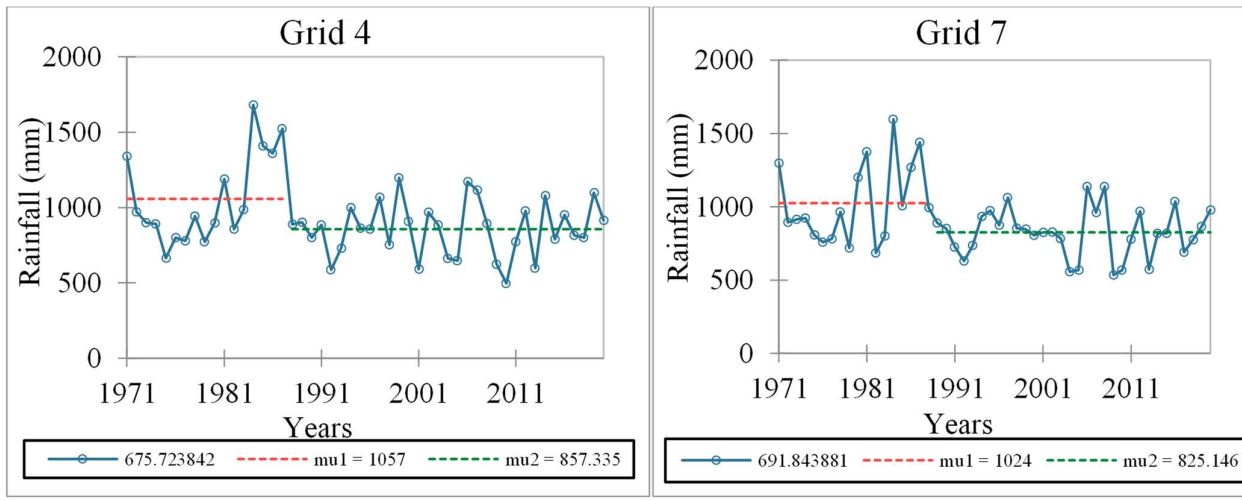

Fig. 5: Change year in the SW-Monsoon rainfall series in G4 by Buishand's test (mu1 and mu2 represent the mean rainfall before and after the change point). Changing year in the SW-Monsoon rainfall series in G7 by Buishand's test.

deficiency from the mean annual rainfall was observed at G15 with a percentage change of -34.41, followed by G10 (-30.61 %), and G5 (-25.83 %). A slight increase in rainfall from the mean annual was observed at Grid 6 (0.25 %) and G9 (2.91 %). A similar change was observed in monsoon rainfall, with the highest deficiency at G10 (-28.29%), followed by G15 (-27.99%) and G5 (-26.76%). Deficiencies were observed in the monsoon rainfall compared to the mean at other grids, except for G3, G9, and G17, where a slight increase was observed. A percentage increase from the mean was observed at all grids except grids 4 and 10 for the pre-monsoon season (Fig. 6). These grids may have experienced meteorological anomalies such as dry winds, insufficient convective triggers, or shadowing effects caused by nearby geographical features. The highest increment occurred in G9 (88.09%), whereas the lowest occurred in G15 (9.57%). The significant increase at G9 suggests the potential influence of localized convectional activities, where heating patterns during the pre-monsoon period result in increased rainfall. Variations in topography, such as the presence of elevated regions or valleys, may affect rainfall distribution. Grids with less development may exhibit enhanced rainfall owing to lower heat retention and increased surface evaporation, which supports the formation of convective rain. In the post-monsoon season, low rainfall was observed across all grids. G9 showed the highest deficiency (-75.40%), followed by G8 (-69.34%) and G17 (-63.60%). The least deficient grids were G13 (-11.30%), G12 (-19.96%), and G6 (-22.54%), respectively. Inconsistent monsoon withdrawal can reduce post-monsoon rainfall. The post-monsoon season often sees rainfall influenced by cyclonic systems, which may have been less active or bypassed the region. G9's extreme deficiency may be related to specific local factors, such as a significant decrease in moisture-laden winds or geographical barriers that disrupt cloud formation. This study indicates that a combination of meteorological, topographical, and anthropogenic factors influences rainfall variability across grids. Seasonal shifts in wind patterns, moisture availability, and disturbance tracks likely contributed to the observed changes in percentage. Grids with high variability (e.g., G9 and G15) may require further investigation to mitigate the impacts of rainfall deficits or excesses.

4.4.2 Trend Analysis and Change Percentage for TS2 (1970-1990)

The Mann-Kendall test was applied to the monthly rainfall data for different periods of the second time series (1970-1990) for all grids, and their corresponding Z values. It was observed that all grids exhibited some trends, either positive or negative, in different periods, except for Grid 10, which showed no trend for annual periods, and Grid 1, which showed no trend in the pre-monsoon periods. No other grids exhibited any significant positive or negative trends in any period, except G17, which exhibited a significant positive trend during the monsoon season with a Z value of 1.99. The results also show the percentage change based on the

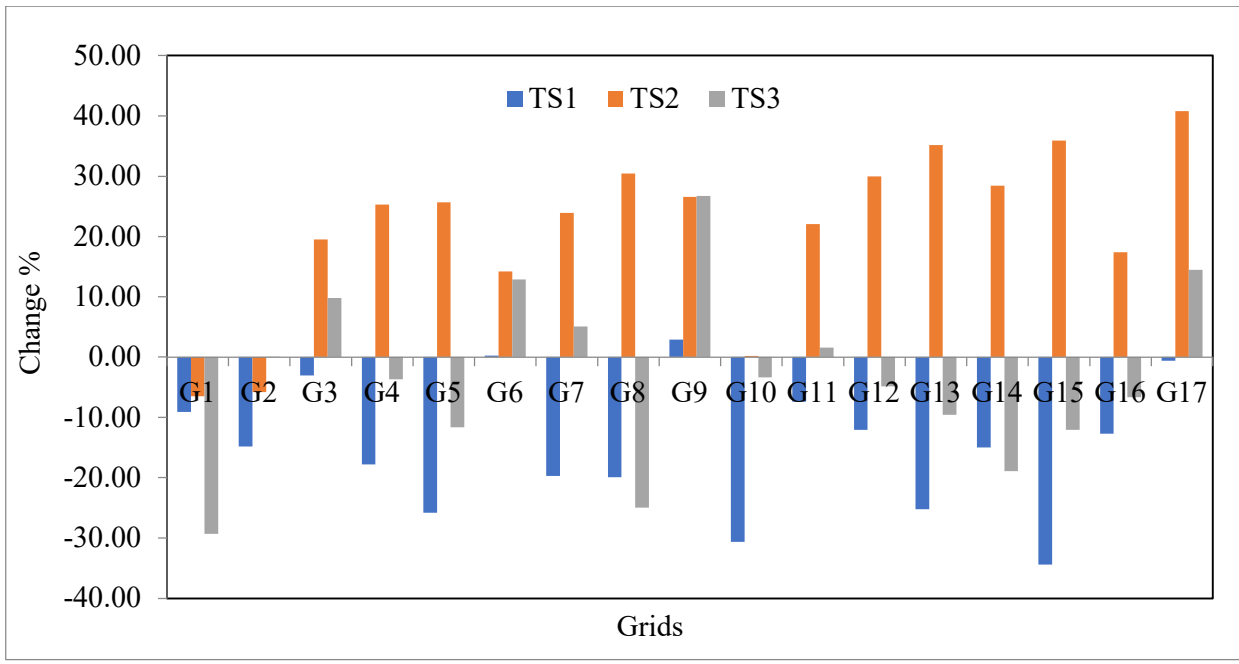

Fig. 6: Percentage change in annual rainfall for different time series of all data grids.

sen-slope value. Based on the observations, it was identified that periods such as annual and monsoon showed an increase in rainfall at all grids, except for G1 and G2, where a slight decrease in rainfall was observed. The highest increase in annual rainfall from the mean was observed at G17, with a percentage change of 40.78, whereas the lowest increment was observed at grid 10, with a change of 0.21%. Similarly, for monsoon periods, G17 was identified as the grid with the highest increment in rainfall from the mean, with a change of 50.76%, and a change of 2.66%; grid 10 was observed as the grid with the lowest increment. Correspondingly, the highest percentage change for the pre-monsoon period, which showed an increase in rainfall from the mean at all 17 grids, was observed at G5 with a value of 100.47%. The lowest increment was observed in Grid 1, with a change of 0.81 percent. In the post-monsoon period, grids G4, G13, and G15 exhibited an increase in rainfall, with percentage values of 5.34, 37.80, and 5.08, respectively. In contrast, the remaining grids showed a decrease in rainfall from the mean value. The most severe drought in post-monsoon rainfall was observed in G10, with a value of -92.44%, and the lowest deficiency was observed in G5, with a change percentage value of -6.03. From the same table, similar Fig.s have been observed for the winter season, where each grid shows a deficiency in rainfall, with the highest decrement observed at G9, at a value of -102.04%, and the lowest at G15, with a change of -21.11%.

4.4.3 Trend Analysis and Change Percentage for TS3 (1991-2020)

The Mann-Kendall test was applied to the third time series (1991-2020), and the corresponding Z values, along with the percent change in rainfall from the mean. Positive or negative trends were observed at different grids for different periods, except at G2 during the annual, G3 and G11 during the monsoon, G13 during the post monsoon, and G16 during the winter, where no trend has been observed. Moreover, no significant trends were observed in the annual, monsoon, post-monsoon, or winter periods. In contrast, only a few significant trends were observed during the pre-monsoon period at G9, G16, and G17, with Z values of 2.82, 2.19, and 2.32, respectively. Additionally, during the pre-monsoon periods, every grid exhibited positive periods, except for Grid 12, where a slight negative trend was observed. Conversely, during the post-monsoon periods, negative trends were observed at all grids except grids 6 and G13. The annual periods for TS3 showed a mixed result of decrement and increment in rainfall from the mean, with a maximum increment of 26.75% at G9 and a minimum increment of 0.03% at G2. In comparison, the maximum deficiency of rainfall has been observed at G1, with a percentage change of -29.29%, and the minimum deficiency was -3.67 % at G4. Similarly, during the monsoon period, a maximum increment of 25.47% was observed at G9, whereas G7 observed a minimum increment in rainfall, with a change of 0.64%. In contrast, as positive trends were observed at different grids during the pre-monsoon period, the highest increment was observed at G9, with a change of 123.48%, and the lowest increment of 3.81% was observed at G11. Correspondingly, during the post-monsoon period, negative trends were observed in all grids except G6 and G13. Specifically, a 1% change was observed at G6, whereas no trend was observed at G13. In comparison, the highest deficiency was observed at G4, with a change percentage of -82.08%, and the minimum deficiency was observed at G12, with a change percentage of -0.63%. In addition, during the winter period, no change in rainfall was observed at G15 and G16, whereas the highest increment was found at G2, with a change percentage of 35.33%. G8 showed a 1.07% change. In contrast, the highest deficiency was observed at G10, with a change percentage of -44.40%, whereas the minimum deficiency was observed at G12, with a change percentage of -3.92%.

4.5 Drought Variability in the Study Region

Precipitation patterns, climate variability, and anthropogenic activities influence drought variability in the semi-arid climatic region of Bihar. The region has experienced significant shifts in rainfall patterns over the past century, with increased drought and flood frequency and intensity due to climate change (Rashiq et al. 2024, Sharma & Priya 2023). The return periods of droughts, drought severity, and number of drought years for annual and seasonal (SW monsoon) rainfall, respectively, for the entire study period (1970-2020). Thus, it was clear that for G1, moderate droughts occurred during the years 1981, 1992, 2001, 2004, 2005, 2017, and 2018, whereas severe drought occurred in 2009 for annual rainfall. Similarly, for seasonal rainfall, moderate droughts were observed in 1981, 1983, 1992, 2001, 2004, 2005, and 2010, whereas severe droughts occurred in 2009 and 2013. The return period of moderate drought is approximately one drought in six to seven years, whereas for severe drought, it is one drought in 51 years for both annual and seasonal rainfall. For the annual time series data, the G1, (G13), G15, and G17 grids showed severe droughts during 2009, (1975, 2004), 1992, and 2005, respectively. G15 experienced almost one drought every 3 to 4 years. Similarly, for the SW monsoon time series data, grids (G1), (G13), and (G17) showed severe droughts during (2013,2009), (1975, 2004), and 2005, respectively. G17 suffered almost one drought every 3–4 years. The study revealed that the probability of receiving at least 75% of the average annual rainfall across different grids in the division ranged between 80.8% and

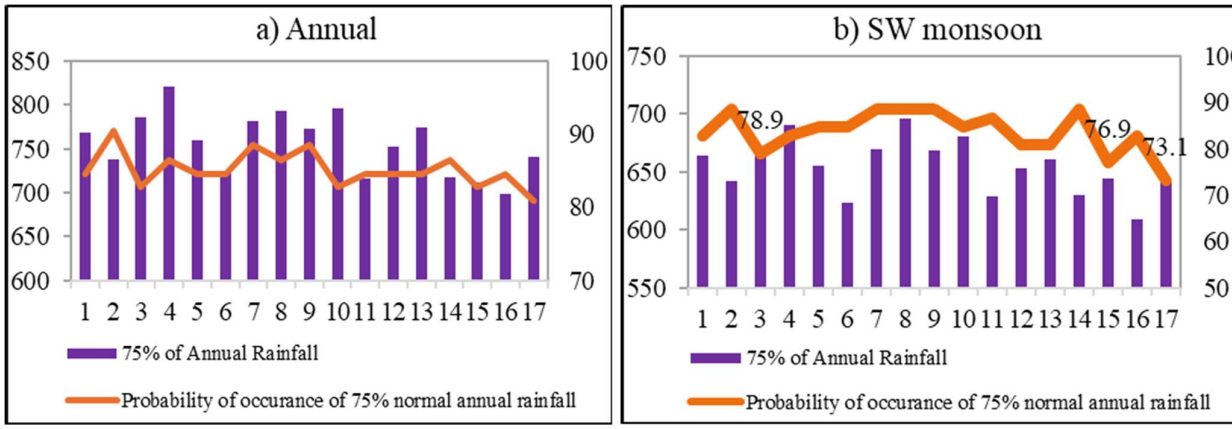

Fig. 7: Probability of the occurrence of a. annual rainfall and b. Southwestern monsoon rainfall (mm).

90.4%. Because the probability remained above 80% in all grids, none of them could be classified as drought-prone (Fig. 7a). However, when examining the probability distribution of southwest monsoon rainfall, the chances of receiving 75% of the normal rainfall varied from 73.1% to 88.5% across the grids (Fig. 7b). Within the Magadh Division, three grids, G3 (78.9%), G15 (76.9%), and G17 (73.1%), fell below the 80% threshold, indicating that these locations are vulnerable to drought conditions. A previous study (Rashiq et al. 2024) revealed significant variability in seasonal rainfall patterns in Bihar, with a notable change in pre-monsoon and post-monsoon rainfall observed in the second epoch (1961–2020). It highlights the significant alterations in rainfall patterns, with extreme weather events, which have led to concerns regarding floods and droughts in the study region.

5. CONCLUSIONS

This study examined rainfall variability, including trends in annual, seasonal, and extreme rainfall, as well as shifts in rainfall patterns, across the Magadh region of Bihar, India. The analysis revealed significant variations in rainfall patterns over time and space, characterized by a distinct change point that reflected shifts in trends and characteristics. In particular, there was a pronounced change in seasonality across all seasons, with the monsoon and post-monsoon periods showing the most substantial shifts, emphasizing the evolving dynamics of rainfall in the region. These findings suggest that rapid urbanization and climate change are likely driving these changes. This study also emphasizes the significance of understanding how decadal climate variability influences regional rainfall patterns. These climate drivers may intensify the frequency and severity of natural disasters, such as droughts, which could worsen water scarcity and create challenges for agriculture in the Magadh region of Bihar. Furthermore, the findings of this study have broader implications for understanding the complex relationship between rainfall variability and drought trends in monsoon-dependent regions. Moving forward, research should prioritize the integration of high-resolution climate models, remote sensing technologies, and ground-based observations to gain a deeper understanding of spatiotemporal aspects of rainfall changes. Additionally, it is vital to incorporate socioeconomic and policy considerations to promote sustainable water resource management and reduce disaster risks in vulnerable areas, such as Magadh. These insights can serve as a foundation for policymakers, urban planners, and stakeholders to develop effective strategies to enhance climate resilience and mitigate the impacts of extreme rainfall events and droughts on agriculture, water resources, and livelihoods.

6. ACKNOWLEDGEMENTS

We extend our gratitude to the Indian Meteorological Department (IMD) for providing the meteorological data used in this research.

7. REFERENCES

Anil, S.S. and Sasi, M., 2025. Spatio-temporal analysis of aridity trends and shifts in Karnataka over 63 years (1958-2020): insights into climate adaptation. *Nature Environment & Pollution Technology*, 24(2), pp.1-12. [DOI]

Asare-Nuamah, P. and Botchway, E., 2019. Understanding climate variability and change: analysis of temperature and rainfall across agroecological zones in Ghana. *Heliyon*, 5(10), pp.12-20. [DOI]

Ashok, K., Guan, Z., Saji, N.H. and Yamagata, T., 2004. Individual and combined influences of ENSO and the Indian Ocean dipole on the Indian summer monsoon. *Journal of Climate*, 17(16), pp.3141-3155. [DOI]

Buishand, T.A., 1982. Some methods for testing the homogeneity of rainfall records. *Journal of hydrology*, *58*(1-2), pp.11-27. [DOI]

Chong, K.L., Huang, Y.F., Koo, C.H., Ahmed, A.N. and El-Shafie, A., 2022. Spatiotemporal variability analysis of standardized precipitation indexed droughts using wavelet transform. *Journal of Hydrology*, 605, p.127299. [DOI]

Dash, S.K., Jenamani, R.K., Kalsi, S.R. and Panda, S.K., 2007. Some evidence of climate change in twentieth-century India. *Climatic Change*, 85(3), pp.299-321. [DOI]

Gogoi, K. and Rao, K.N., 2022. Analysis of rainfall trends over Assam, North East India. *Current World Environment*, 17(2), pp.435-446. [DOI]

Guhathakurta, P., Bandgar, A., Menon, P., Prasad, A.K., Sangwan, N. and Advani, S.C., 2020. Observed Rainfall Variability and Changes over Mizoram State. Meteorological Department, Ministry of Earth Sciences, New Delhi, pp.1-50.

Gupta, N., Mahato, P.K., Patel, J., Omar, P.J. and Tripathi, R.P., 2022. Understanding the trend and the variability of rainfall and temperature over Patna (Bihar). In: *Current Directions in Water Scarcity Research*, Vol. 7, pp.533-543. Elsevier. [DOI]

Keyantash, J. and Dracup, J.A., 2002. The quantification of drought: an evaluation of drought indices. *Bulletin of the American Meteorological Society*, 83(8), pp.1167-1180. [DOI]

Khaniya, B., Jayanayaka, I., Jayasanka, P. and Rathnayake, U., 2019. Rainfall trend analysis in Uma Oya basin, Sri Lanka, and future water scarcity problems in perspective of climate variability. *Advances in Meteorology*, 2019(1), pp.363-378. [DOI]

Kumar, S., Sarthi, P.P., Barat, A. and Sinha, A.K., 2022. Variability in meteorological droughts as a pivotal mechanism for rice production over the middle Gangetic plains. *Paddy and Water Environment*, 20(4), pp.499-516. [DOI]

Larsen, M.L. and Schönhuber, M., 2018. Identification and characterization of an anomaly in two-dimensional video disdrometer data. *Atmosphere*, 9(8), p.315. [DOI]

Mishra, R.K., 2020. A study of climatic conditions in the Punpun basin of the Magadh region, Bihar, India. *International Journal of Advanced Research and Development*, 5(5), pp.6-9.

Nyembo, L.O., Larbi, I. and Rwiza, M.J., 2021. Analysis of spatio-temporal climate variability of a shallow lake catchment in Tanzania. *Journal of Water and Climate Change*, 12(2), pp.469-483. [DOI]

Pawar, U. and Rathnayake, U., 2022. Spatiotemporal rainfall variability and trend analysis over the Mahaweli Basin, Sri Lanka. *Arabian Journal of Geosciences*, 15(4), p.370. [DOI]

Pettitt, A.N., 1979. A non-parametric approach to the change-point problem. *Journal of the Royal Statistical Society: Series C (Applied Statistics)*, *28*(2), pp.126-135. [DOI]

Praveen, B., Talukdar, S., Shahfahad, Mahato, S., Mondal, J., Sharma, P. and Rahman, A., 2020. Analyzing trends and forecasting of rainfall changes in India using non-parametric and machine learning approaches. *Scientific Reports*, 10(1), p.10342. [DOI]

Rashiq, A., Kumar, V. and Prakash, O., 2024. A spatiotemporal assessment of the precipitation variability and pattern, and an evaluation of the predictive reliability, of global climate models over Bihar. *Hydrology*, 11(4), p.50. [DOI]

Ribeiro, S., Caineta, J. and Costa, A.C., 2016. Review and discussion of homogenization methods for climate data. *Physics and Chemistry of the Earth, Parts A/B/C*, 94, pp.167-179. [DOI]

Sahana, M., Rehman, S., Ahmed, R. and Sajjad, H., 2021. Analyzing climate variability and its effects in Sundarban Biosphere Reserve, India: reaffirmation from local communities. *Environment, Development and Sustainability*, 23, pp.2465-2492. [DOI]

Saharwardi, M.S., Kumar, P., Dubey, A.K. and Kumari, A., 2022. Understanding the spatiotemporal variability of drought in recent decades and its drivers over-identifies homogeneous regions of India. *Quarterly Journal of the Royal Meteorological Society*, 148(747), pp.2955-2972. [DOI]

Sarkar, U.K., Roy, K., Naskar, M., Karnatak, G., Puthiyottil, M., Baksi, S. and Das, B.K., 2021. Assessing vulnerability of freshwater minnows in the Gangetic floodplains of India for conservation and management: anthropogenic or climatic change risk? *Climate Risk Management*, 33, p.100325. [DOI]

Sharma, M.R. and Priya, S., 2023. Long-term assessment of precipitation behavior in Bihar (1901-2021): patterns, trends and observed variability. *Current World Environment*, 18(2), pp.662. [DOI]

Singh, A., Kumar, R., Kumar, R., Pippal, P.S., Sharma, P. and Sharma, A., 2024. Delineation of groundwater potential zone using geospatial tools and analytical hierarchy process (AHP) in the state of Uttarakhand, India. *Advances in Space Research*, 73(6), pp.2939-2954. [DOI]

Singh, P., Mall, R.K. and Singh, K.K., 2024. District-wise spatiotemporal analysis of precipitation trend during 1900-2022 in Bihar state, India. *Mausam*, 75(4), pp.1059-1070. [DOI]

Sudriani, Y., Sebestyén, V. and Abonyi, J., 2023. Surface water monitoring systems—the importance of integrating information sources for sustainable watershed management. *IEEE Access*, 11, pp.36421-36451. [DOI]

Tesfaye, K., Aggarwal, P.K., Mequanint, F., Shirsath, P.B., Stirling, C.M., Khatri-Chhetri, A. and Rahut, D.B., 2017. Climate variability and change in Bihar, India: challenges and opportunities for sustainable crop production. *Sustainability*, 9(11), p.1998. [DOI]

Tiwari, D.K. and Sarthi, P.P., 2024. Trends in the rainfall pattern over the Gangetic Plain. *Current World Environment*, 19(1), pp.156. [DOI]

Trenberth, K.E., 2011. Changes in precipitation with climate change. *Climate Research*, 47(1-2), pp.123-138. [DOI]

Vahab, S. and Sankaran, A., 2025. Multifractal applications in hydro-climatology: a comprehensive review of modern methods. *Fractal and Fractional*, 9(1), p.27. [DOI]

Vicente Serrano, S., Domínguez-Castro, F., Murphy, C., Hannaford, J., Reig, F., Pena-Angulo, D. and El Kenawy, A., 2020. Long-term variability and trends in meteorological droughts in Western Europe (1851-2018). *International Journal of Climatology*, 41(S1), pp.E690-E717. [DOI]

Warwade, P., Tiwari, S., Ranjan, S., Chandniha, S.K. and Adamowski, J., 2018. Spatio-temporal variation of rainfall over Bihar State, India. *Journal of Water and Land Development*, 42(1), pp.1-10. [DOI]

Wen, X., Tu, Y.H., Tan, Q.F., Li, W.Y., Fang, G.H., Ding, Z.Y. and Wang, Z.N., 2020. Construction of 3D drought structures of meteorological drought events and their spatio-temporal evolution characteristics. *Journal of Hydrology*, 590, p.125539. [DOI]

Wijngaard, J.B., Klein Tank, A.M.G. and Können, G.P., 2003. Homogeneity of 20th century European daily temperature and precipitation series. *International Journal of Climatology: A Journal of the Royal Meteorological Society*, 23(6), pp.679-692. [DOI]

Wudineh, F.A., Moges, S.A. and Kidanewold, B.B., 2022. Detecting hydrological variability in precipitation extremes: application of reanalysis climate product in data-scarce Wabi Shebele Basin of Ethiopia. *Journal of Hydrologic Engineering*, 27(2), 05021035. [DOI]

Yildirim, G. and Rahman, A., 2022. Homogeneity and trend analysis of rainfall and droughts over Southeast Australia. *Natural Hazards*, 112(2), pp.1657-1683. [DOI]

Yürekli, K., 2015. Impact of climate variability on precipitation in the Upper Euphrates–Tigris Rivers Basin of Southeast Turkey. *Atmospheric Research*, 154, pp.25-38. [DOI]

Zakwan, M. and Ara, Z., 2019. Statistical analysis of rainfall in Bihar. *Sustainable Water Resources Management*, 5, pp.1781-1789. [DOI]

Zhang, Q., Li, J., Singh, V.P. and Xiao, M., 2013. Spatio-temporal relations between temperature and precipitation regimes: implications for temperature-induced changes in the hydrological cycle. *Global and Planetary Change*, 111, pp.57-76. [DOI]